Cancer Chemother Pharmacol (2007) 59:397–405
DOI 10.1007/s00280-006-0294-6

ORIGINAL ARTICLE

MZ3 induces apoptosis in human leukemia cells

Liang Fang · Qiaojun He · Yongzhou Hu · Bo Yang

Received: 4 May 2006 / Accepted: 18 July 2006 / Published online: 10 August 2006

Abstract
Purpose 4-(4-Bromophenyl)-2,3-dihydro-*N*,3-bis(3,4,5-trimethoxyphenyl)-2-oxoidmi-dazole-1-carboxamide (MZ3) is one of the synthesized combretastatin-A-4 analogues and has been reported that it displayed a promising specific activity against leukemia cell lines. Our purpose was to investigate the mechanism of MZ3's cytotoxicity.
Methods Cytotoxicity was measured by MTT method, apoptosis was measured by flow cytometry. DNA fragmentation was tested by agarose gel electrophoresis. Mitochondrial membrane potential ($\Delta\Psi m$) was detected by JC1 staining and flow cytometry, while intracellular reactive oxygen species (ROS) was detected by 5-(and-6)-carboxy-2′-7′-dichlorofluorescin diacetate staining and flow cytometry. Protein expression was analyzed by western blotting. In vivo activity of MZ3 was assayed through severe combined immunodeficiency (SCID) mice model of human leukemia engrafts.
Results MZ3 exhibited high anti-cancer activity in six leukemia cell lines, including two drug-resistant cell lines. MZ3 induced DNA fragmentation, and caused an elevation of ROS and a loss of $\Delta\Psi m$ in HL60 cells. MZ3 also induced the activation of caspase-3, influenced the expression of Bcl-2 family members, MAPKs and other proteins relative to mitochondria-induced apoptosis. In addition, *N*-acetylcysteine cannot inhibit HL60 cell apoptosis caused by MZ3. Furthermore, a prolonged survival time was observed after treatment with MZ3 in SCID mice model of human leukemia engrafts.
Conclusions MZ3 is a potent compound against leukemia cell lines both in vitro and in vivo, and the mitochondrial pathway mediated by Bcl-2 protein family and MAPKs might be involved in signaling MZ3-induced apoptosis.

Keywords Leukemia · Bcl-2 protein family · MAPKs · Caspases · Mitochondria

Abbreviations

$\Delta\Psi m$	Mitochondrial membrane potential
SCID	Severe combined immunodeficiency
MST	Median survival time
ROS	Reactive oxygen species
JC-1	5,5′,6,6′-Tetrachloro-1,1′,3,3′-tetraethylbenzimidazol-carbocyanine iodide
Carboxy- DCFDA	5-(and-6)-Carboxy-2′-7′-dichlorofluorescin diacetate
Apaf-1	Apoptosis-activating factor 1
IAPs	Inhibitors of apoptosis proteins
MZ3	4-(4-Bromophenyl)-2,3-dihydro-*N*,3-bis (3,4,5-trimethoxyphenyl)-2-oxoidmi-dazole-1-carboxamide
CTX	Cyclophosphamide
NAC	*N*-Acetylcysteine

Introduction

Combretastatin-A-4 has been reported as one of the most potent anti-tumor agents of *Combretum Caffrum*, because of its simple structure and strong cytotoxicity

L. Fang · Q. He · Y. Hu · B. Yang (✉)
Institute of Pharmacology and Toxicology,
School of Pharmaceutical Sciences, Zhejiang University,
353# Yan'an Rd., Hangzhou, Zhejiang 310031, China
e-mail: yang924@zju.edu.cn

against a variety of human cancer cells, including multidrug-resistant cancer lines [1]. Numerous studies on the structure–activity relationships of combretastatin-A-4 have demonstrated that the *cis*-orientation between the diaryl groups was essential for its strong cytotoxicity. This finding prompted the design and synthesis of a number of *cis*-restricted analogues of combretastatin-A-4 [2–5]. 4-(4-Bromophenyl)-2,3-dihydro-*N*,3-bis(3,4,5-trimethoxyphenyl)-2-oxoidmi-dazole-1-carboxamide (MZ3, Fig. 1) is one of the synthesized combretastatin-A-4 analogues. Although it displayed a promising specific activity against leukemia cell lines in previous reports [5], the mechanism of MZ3's cytotoxicity is not clear.

Recent investigations have demonstrated that the mitochondrial dysfunction is involved in apoptosis [6–8]. An increase of reactive oxygen species (ROS) [9, 10] and a consequent loss of mitochondrial membrane potential ($\Delta\Psi m$) [11, 12] were reported as typical phenomena in the process of apoptosis related to mitochondria [13, 14]. It is known that mitochondria-mediated apoptosis is regulated by two major pathways. The death receptors on the cell surface can affect the mitochondria indirectly by regulation of MAPKs [15] and the convergence of the signaling at the mitochondria can influence the mitochondria directly by regulation of Bcl-2 protein family [16–19].

In this article, we reported the anti-leukemia effects of MZ3 on six leukemia cell lines in vitro, including two drug-resistant cells, and on severe combined immunodeficiency (SCID) mice model of human leukemia engrafts in vivo. In addition, the involvement of mitochondrial dysfunction in MZ3-induced apoptosis was investigated.

Materials and methods

Drugs and chemicals

MZ3 was synthesized according to the previous report [5], dissolved in DMSO (8.0 mM stock solution) and stored at -20°C. For in vivo test, MZ3 and cyclophosphamide (CTX, Shanghai Hualian Pharmaceutical Co., Ltd, Shanghai, China) were freshly dissolved in injectable oleum camelliae or saline, respectively, to make a final concentration of 2.0 mg/ml. The mitochondrial fluorescent probe 5,5′,6,6′-tetrachloro-1,1′,3,3′-tetraethylbenzimidazol-carbocyanine iodide (JC-1) and the 5-(and-6)-carboxy-2′-7′-dichlorofluorescin diacetate (carboxy-DCFDA) were purchased from Molecular Probes (Eugene, OR, USA). Stock solutions of JC-1 (2.0 mg/ml) and carboxy-DCFDA (15.0 mM) were dissolved in DMSO and stored at -20°C. The thiol anti-oxidant *N*-acetylcysteine (NAC) was purchased from Sigma (St Louis, MO, USA). NAC was freshly dissolved in medium at a final concentration of 200.0 μM, the pH adjusted to 7.4, and sterilized by 0.22 μM filtration. The primary antibodies to caspase-3, Bcl-2, Bax, ERK1/2, p38, JNK, p-ERK1/2, p-p38, p-JNK, XIAP, PARP, α-tubulin and β-actin, and HRP-labeled secondary anti-goat, anti-mouse and anti-rabbit antibodies were purchased from Santa Cruz Biotechnology (Santa Cruz, CA, USA). ECL, a western blot detection reagent, was purchased from Pierce Biotechnology (Rockford, IL, USA).

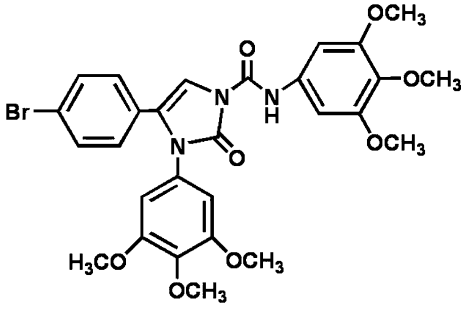

Fig. 1 Structure of MZ3

Cell lines

The human leukemia cell lines (K562, HL60, and Molt-4) were obtained from ATCC, and two drug-resistant cell lines (K562R, HL60R) [20] and an acute promyelocytic leukemia line (NB4) were endowed by Shanghai Institutes for Biological Sciences (Chinese Academy of Sciences). The K562R displayed 76.1-fold resistance to vincristine and HL60R displayed 26.9-fold resistance to daunorubicin compared with their corresponding parental cells. All cell lines were maintained in RPMI-1640 medium (Gibco, Grand Island, NY, USA) with 10% heat-inactivated newborn calf serum (NCS, Gibco, Grand Island, NY, USA) at 37°C in 20% O_2.

Cytotoxicity assay

The cytotoxic activity of MZ3 on six leukemia cell lines was measured using the MTT assay. After treatment (0.25–16.0 μM MZ3 for 72 h) in 96-well plates, MTT solution (5.0 mg/ml in RPIM-1640, Sigma, St Louis, MO, USA) was added (10.0 μl/well), and plates were incubated for a further 4 h at 37°C. The purple formazan crystals were dissolved in 100.0 μl DMSO. After 5 min, the plates were read on an automated microplate spectrophotometer (Bio-Tek Instruments, Winooski, VT, USA) at 570 nm. For some assays, NAC was added to a final concentration of 200.0 μM, 3 h before the addition of MZ3. Assays were performed in triplicate on three

independent experiments. The concentration of drug inhibit for 50% of cells (IC_{50}) was calculated using the software of dose–effect analysis with microcomputers.

Flow cytometric analysis of DNA content

HL60 cells (2×10^6) were collected by centrifugation, washed with PBS, and fixed with 70% ethanol. The fixed cells were harvested by centrifugation at 200*g* for 10 min and resuspended in 100.0 ml of PBS containing 50.0 mg/ml RNase (Amersco, Solon, OH, USA), then incubated at 37°C for 1 h. After incubation, the cells were stained with 200.0 mg/ml propidium iodide (PI, Sigma, St Louis, MO, USA) at 4°C for 30 min. The fluorescence of cell (2×10^4) was measured with FACSCalibur (Becton Dickinson, Lincoln Park, NJ, USA) [21].

Electrophoretic analysis of DNA fragmentation

HL60 cells (2×10^6) were lysed in 200.0 ml lysis buffer (10.0 mM EDTA; 50.0 mM Tris–HCl, pH 8.0; 0.5% sodium lauryl sulfate; 100.0 mg/ml proteinase K) at 37°C for 12 h, then incubated with RNase (50.0 mg/ml) at 37°C for an additional 1 h. After incubation, DNA in the lysate was extracted with equal volume of phenol/chloroform/isoamyl alcohol (25:24:1), then with chloroform. DNA was precipitated with two volumes of ethanol in the presence of 0.3 M sodium acetate. After centrifugation at 12,000*g* for 15 min, the DNA pellets were washed with 70% ethanol, air-dried, and resuspended in 20.0 ml TE (10.0 mM Tris–HCl and 1.0 mM EDTA, pH 8.0). DNA was separated on 1.5% agarose gels containing 0.5 mg/ml ethidium bromide and photographed by Bio-Rad GD2000 (Bio-Rad, Hercules, CA, USA) [22].

Assessment of ΔΨm

The harvested cells (2×10^6) were resuspended in 0.5 ml of complete medium containing 10.0 μg/ml of JC-1 for 10 min at 37°C. JC-1 is a cationic dye that exhibits potential-dependent accumulation in mitochondria, indicated by a fluorescence emission shift from green (525 ± 10 nm) to red (610 ± 10 nm). Samples (1×10^4 cells/sample) were analyzed by FACSCalibur using an argon laser (488 nm). Mitochondria depolarization is specifically indicated by a decrease in the red to green fluorescence intensity ratio [21].

Detection of intracellular ROS

The production of intracellular ROS was measured in the HL60 cell line using the oxidation-sensitive fluorescent dye carboxy-DCFDA. An increase in green fluorescence intensity is used to quantify the generation of intracellular ROS. After adding carboxy-DCFDA at a final concentration of 15.0 μM to the culture medium, the cells were incubated at 37°C for an additional 30 min, harvested, washed with PBS, and measured immediately by FACSCalibur using an argon laser at 488 nm and a 525-nm band pass filter [23].

Western analysis

Proteins of HL60 cells were extracted in radioimmunoprecipitation assay buffer (50.0 mM NaCl, 50.0 mM Tris–HCl, 1.0% Triton X-100, 1.0% sodium deoxycholate, and 0.1% SDS) and 40.0–80.0 μg of total protein was loaded per lane. Proteins were fractionated on 10–15% Tris–glycine pre-cast gels, transferred to nitrocellulose membrane (Pierce Biotechnology, Rockford, IL, USA), and probed with primary antibodies and then HRP-labeled secondary antibodies. Proteins were visualized using ECL (Pierce Biotechnology).

Measurement of in vivo activity

To establish SCID mice model of human leukemia engrafts, female SCID mice (6- to 7-week-old) were chosen and transplanted by tail vein injection with 1×10^7 HL60 human leukemia cells that had been washed and seeded into fresh medium 12 h prior to use [24]. The day after transplantation of the HL60 cells, mice were administrated (i.m.) with 10.0 mg/kg MZ3 or 10.0 mg/kg CTX daily for ten consecutive days. Then the survival curves were obtained by monitoring the length of their survival time.

Statistics

Significance of mean values was determined by unpaired two-tailed Student's *t*-test. Significance of dose–response curve was detected by ANOVA.

Results

Cytotoxicity of MZ3

The anti-leukemia activity of MZ3 was determined on six human leukemia cell lines, including HL60, K562, Molt-4, NB4, and two drug-resistant cell lines, HL60R and K562R. As shown in Table 1, MZ3 has anti-leukemia activity on all six cell lines, and IC_{50} values of MZ3 for all six leukemia cells are <8.0 μM in a dose-dependent manner. Particularly, MZ3 shows strong cytotoxic

effect on two drug-resistant cell lines. The results suggest that MZ3 has promising anti-leukemia activity.

MZ3-induced apoptosis

DNA fragmentation is a common feature of apoptotic cell death. Electrophoretic analysis of DNA (Fig. 2a) shows that exposure of HL60 cells to MZ3 (4.0, 8.0, 16.0 μM) for 24 h resulted in a characteristic fragmentation of DNA at intranucleosomal sites, a biochemical hallmark of apoptosis. In addition, the results of flow cytometric analysis of DNA content (Fig. 2b) further shows that MZ3 induced 2.5–85.4% increases in the DNA fragments when HL60 cells were treated with MZ3 (4.0 μM) for 6–72 h.

Table 1 Cytotoxicity of MZ3 on human leukemia cell lines

Leukemia origin	Cell line	IC_{50} (μM)
Acute promyelocytic leukemia	NB4	1.16 ± 0.22
Acute lymphoblastic leukemia	Molt-4	4.17 ± 0.39
Chronic myelocytic leukemia	K562	3.38 ± 0.12
Chronic myelocytic leukemia (76.1-fold resistance to vincristine)	K562R	8.00 ± 0.29
Acute promyelocytic leukemia	HL60	2.65 ± 0.19
Acute promyelocytic leukemia (26.9-fold resistance to daunorubicin)	HL60R	3.46 ± 0.48

Cells were exposed with various concentrations (0.25–16.0 μM) of MZ3 for 72 h

Loss of ΔΨm

Loss of ΔΨm leads to release of cytochrome c from mitochondria and consequently trigger other apoptotic factors. We observed ΔΨm in HL60 cell line treated with 8.0 μM MZ3 for 8–24 h by flow cytometry after JC-1 staining. A loss of ΔΨm is specifically indicated by a decrease in the ratio of red to green fluorescence intensity (Fig. 3a). Compared to the corresponding control, MZ3 caused an obvious decrease of ΔΨm in HL60 cells at 16–24-h incubation in a time-dependent manner, and 48.4% cells presented low ΔΨm at 24-h incubation while 2.0% in control group (Fig. 3b).

Increase of ROS

Mitochondria are sensitive to changes in cellular redox state, and ROS can cause mitochondrial dysfunction. HL60 cells were exposed to 8.0 μM MZ3 for 1–4 h prior to staining with carboxy-DCFDA and flow cytometric analysis. A peak of mean green fluorescence (1.7-fold over control) was detected at 2-h treatment with MZ3 (Fig. 4a). Afterward, ROS production showed a decreased trend at 3–4 h after the addition of MZ3 (Fig. 4b). In order to investigate whether the production of ROS is the key matter in MZ3-induced apoptosis. NAC (200.0 μM) was added 3 h before the addition of MZ3 (8 μM for 72 h), and the results

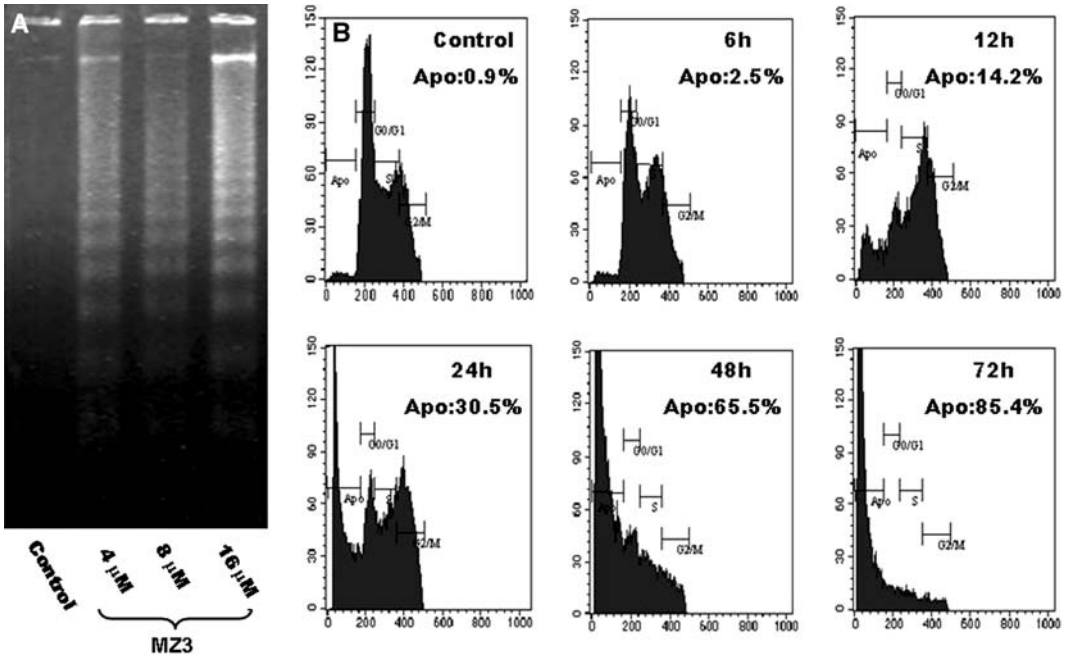

Fig. 2 MZ3-induced apoptosis in HL60 cells. After treatment with MZ3, a characteristic cleavage of DNA was observed (**a**) in HL60 cells. By PI staining and flow cytometry, 2.5–85.4% DNA fragments were detected in HL60 cells treated with MZ3 (**b**)

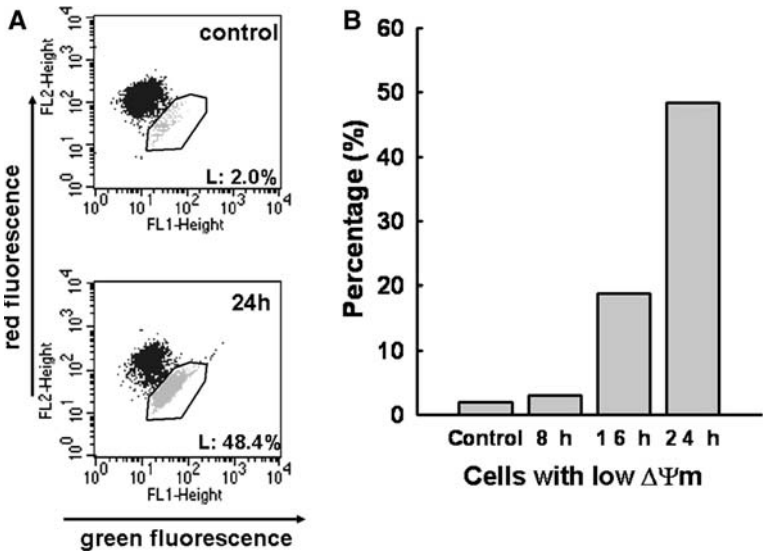

Fig. 3 Loss of ΔΨm caused by MZ3 in HL60 cells. After treatment of MZ3, a loss of ΔΨm in HL60 cell line was detected by flow cytometry after JC-1 staining. The *green fluorescence* intensity indicated the cells with low ΔΨm, while the *red fluorescence* intensity indicated the cells with stable ΔΨm. *L*—cells with low mitochondrial membrane potential

showed that the anti-cancer activity (inhibition rate) of MZ3 to HL60 cells did not decrease, indicating that NAC failed to abrogate cytotoxicity of MZ3 in HL60 cells (Fig. 4c).

Caspase cascade in MZ3-induced apoptosis

In most cases, the activation of caspase cascade accompanies with the apoptosis. The expression of caspase-3, XIAP, and PARP was measured in HL60 treated with MZ3 (8.0 μM, 6–24 h). As shown in Fig. 5, MZ3 (>12-h treatment) obviously decreased procaspase-3 and XIAP protein levels, and induced the cleavage of procaspase-3 and PARP in a time-dependent manner.

Changes of protein expression related to mitochondria

There are many proteins related to the mitochondrial pathway. MAPKs and Bcl-2 family are two major protein families regulating mitochondria on the upstream, and caspase-3 pathway, on the downstream, can be activated after mitochondrial dysfunction. The expression of Bcl-2, Bax, ERK1/2, p38, JNK, p-ERK1/2, p-p38, p-JNK was measured in HL60 treated with MZ3 (8.0 μM, 6–24 h). As shown in Fig. 6a, MZ3 (>12-h treatment) decreased p-ERK and ERK protein levels, increased the expression of p-p38 and p-JNK in a time-dependent manner. Moreover, MZ3 treatment resulted in the decrease of Bcl-2 and increase of Bax (Fig. 6b), with an increase in Bax/Bcl-2 ratio (Fig. 6c).

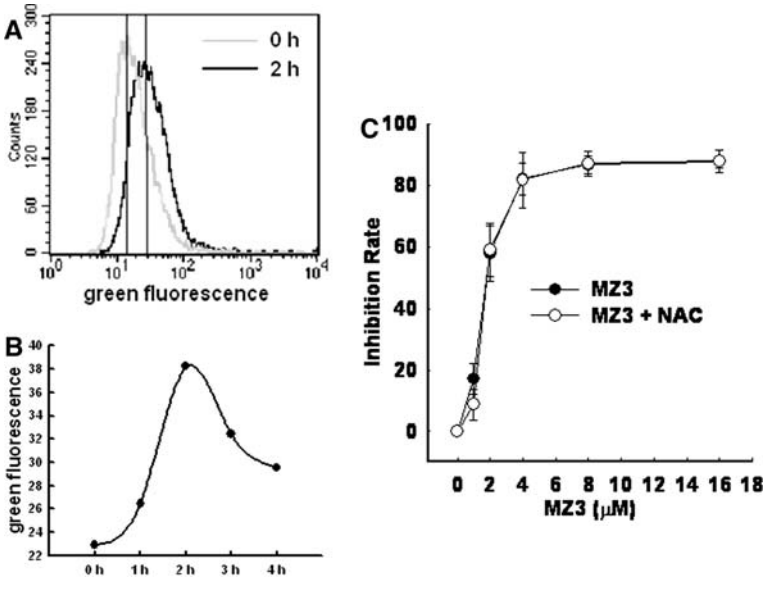

Fig. 4 Increase of ROS after MZ3 treatment in HL60 cells. A 1.7-fold increase in ROS was detected in the cells treated with MZ3 for 2 h (**a**). Afterward, ROS production showed a decreased trend at 3–4 h after the addition of MZ3 (**b**). However, pre-treatment with NAC did not significantly reduce the cytotoxicity (inhibition rate) of MZ3 to HL60 cells (**c**)

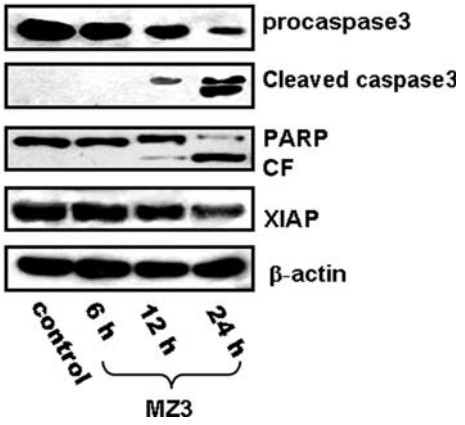

Fig. 5 Caspase-3 (relative protein) expression and apoptosis in HL60 cells treated by MZ3. MZ3 obviously decreased procaspase-3, XIAP protein levels in HL60 cells and induced the cleavage of procaspase-3 and PARP expression in a time-dependent manner

In vivo anti-tumor activity

Severe combined immunodeficiency mice transplanted with HL60 cells were administrated (i.m.) with 10.0 mg/kg MZ3 or 10.0 mg/kg CTX daily for ten consecutive days and the length of their survival time was monitored (Fig. 7). As shown in Fig. 7, the six untreated control animals were all dead by the 20th day after implantation, while the first death occurred in 25th and 26th day in CTX group and MZ3 group, respectively. The MSTs of CTX group and MZ3 group were 26.5 and 33.5 days, respectively, compared with the control group (MST 15 days).

Discussion

MZ3 was modified from combretastatin-A-4 and was reported to have specific cytotoxicity to leukemia cells. Although combretastatin-A-4 was reported as a vascular- and mitosis-targeted agent, after modification, MZ3's structure was fundamentally changed. As a novel compound, this paper focuses on the effect and mechanism of its anti-leukemia characteristics. The analysis of cytotoxicity in vitro indicates that MZ3 is able to inhibit the cell proliferation on all six leukemia cell lines with a time-dependent and dose-dependent manner. Particularly, MZ3 shows strong cytotoxic effect on drug-resistant cell lines, suggesting that it may service as a potential anti-resistant drug. Meanwhile, the DNA fragmentation indicates that cytotoxicity of MZ3 is related to the apoptotic process. In addition, the results that MZ3 (10.0 mg/kg, i.m.) prolonged the survival time of SCID mice transplanted with human leukemia engrafts indicated its anti-leukemia action of MZ3 in vivo.

It has been reported that mitochondria are involved in signaling apoptosis [6–8], and ROS is a powerful activators in loss of ΔΨm [9] and apoptosis [10]. The present study exhibited that MZ3 induced an increase of ROS and a consequent loss of ΔΨm, but NAC failed to inhibit cytotoxicity of MZ3 in HL60 cells, indicating that ROS may not the key matter in this apoptotic process. ΔΨm loss can induce the opening of permeability transition pores in mitochondria, and release cell death-promoting factor, cytochrome c [11, 12], which leads to the formation of a complex consisting of apoptosis-activating factor 1 (Apaf-1) and caspase-9 and initiates

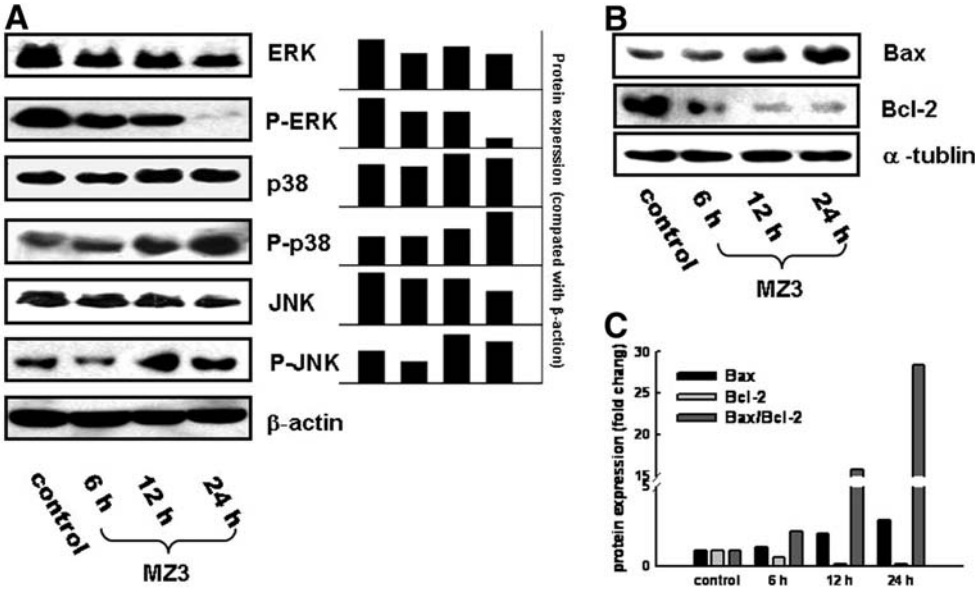

Fig. 6 Protein expression in HL60 cells after MZ3 treatment. MZ3 obviously decreased p-ERK1/2 protein levels in HL60 cells, increased expression of p-p38 and p-JNK in a time-dependent manner (**a**). Moreover, the decrease of Bcl-2 and increase of Bax can be seen in **b**, and the huge increase of Bax/Bcl-2 ratio was shown in **c**

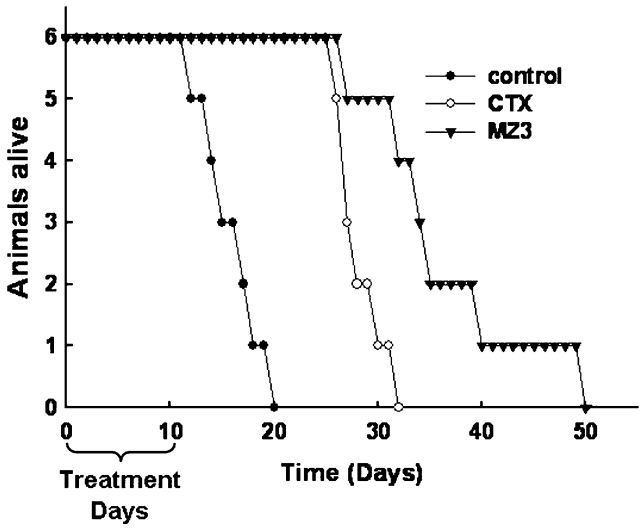

Fig. 7 Survival *curves* of SCID mice transplanted with HL60. Both of MZ3 and CTX prolonged the survival time compared with control group, and survival curves were drawn at the day after transplantation

the proteolytic apoptotic cascade. Therefore, the observation of MZ3-mediated activation of procaspase-3 and subsequent cleavage of its substrate PARP [25] suggested that mitochondrial pathway played a very important role in MZ3-induced apoptosis. Furthermore, the MZ3-caused downregulation of XIAP, one of the inhibitors of apoptosis proteins (IAPs) family [26–28], was detected in HL60 cells. Since the XIAP is able to inhibit activation of caspase-3 to protect cells from apoptosis, the downregulation of XIAP provides an additional documentation that MZ3-induced anti-leukemia is related to activate caspase cascade. Taken together, the present study indicate that MZ3-induced apoptosis is mediated by mitochondrial permeability changes that lead to caspase-dependent cytotoxicity.

Recent investigations have demonstrated that two major pathways are involved in mitochondria-mediated apoptosis. Through convergence of the signaling at the mitochondrial membrane, Bcl-2 protein family [18–21] can influence the mitochondria directly. The Bcl-2 protein family includes proapoptotic members, such as Bax, Bad, and Bcl-Xs, and anti-apoptotic members, such as Bcl-2, Bcl-XL, and Bcl-W. Anti-apoptotic members act as repressors of apoptosis by blocking the release of cytochrome c, whereas proapoptotic members act as promoters. The final action is dependent on the balance between Bcl-2 [29, 30] and Bax [31], and the increase of Bax/Bcl-2 ratio could induce the release of cytochrome c [32, 33]. Our results demonstrated a dramatic increase of Bax/Bcl-2 ratio in HL60 cells treated with MZ3, indicating that the regulation of Bcl-2 protein family expression plays an important role in MZ3-induced apoptosis.

As discussed above, the expression level of Bcl-2 protein family is vitally important to mitochondrial-mediated apoptosis. Furthermore, the activation, deactivation, and translocation are also critical for Bcl-2 protein family to affect the mitochondrial function. MAPKs, a protein family, related to death receptors on the cell surface, can indirectly affect mitochondrial function by interaction with Bcl-2 family and other factors. The MAPK family consists of a superfamily of three parallel signal transduction modules converging on the serine/threonine kinases JNK, ERK, and p38 [15]. These kinases are activated by a variety of stimuli and are intimately involved in diverse cellular processes including responses to DNA damage or osmotic shock, mitogenic stimuli, cell differentiation, and survival [34]. Although exceptions occur, activation of JNK and p38 MAPK are generally associated with induction of apoptosis, whereas ERK exerts cytoprotective effects [35]. As reported, JNK can interface the binding ability of Bcl-2 with Bax and impair anti-apoptotic function of Bcl-2 by phosphorylation [36, 37]. Activation of ERK leads to phosphorylation of several downstream effectors, including protein kinases and transcription factors responsible for regulating genes that enhance cell proliferation and protect from apoptosis [38]. One biochemical link between ERK and Bcl-2 family is regulation of the phosphorylation of Bad. ERK can phosphorylate Bad at Ser112 and then inactivate Bad by sequestering it in the cytosol and preventing its dimerization with Bcl-XL [39]. Furthermore, ERK can regulate Bcl-2 [40] and Bcl-XL [41] protein expression in some cell types. Bax translocation to mitochondria occurs in response to activation of p38 and is an early event in the release of cytochrome c [42]. Inhibition of p38 strongly reduces the UVB-induced formation of sunburn cells and blocks Bax conformational change both in cultured human keratinocytes and in human skin, providing clear evidence for the physiological role of the p38 MAPK–Bax pathway in the removal of precancerous, UVB-damaged keratinocytes [43]. Since JNK, p38, and ERK can only exert their activity after phosphorylation, the upregulation or the downregulation of these phosphorylated proteins indicate the activity of the corresponding proteins. In present study, our results exhibited that MZ3 obviously upregulated p-JNK and p-p38, and downregulated p-ERK and ERK. In contrast, there was little change in the expressions of JNK and p38. These observations suggested that the MAPKs activity may involve in the MZ3-mediated apoptotic process.

In conclusion, all of the data above demonstrated that MZ3 is a potent compound against leukemia cell lines both in vitro and in vivo, and the mitochondrial pathway, mediated by Bcl-2 protein family and MAPKs, might be involved in the activation of caspase cascade to induce cell apoptosis.

Acknowledgments This study received financial support from the National Natural Science Foundation (No. 30400557), the Science and Technology Foundation of Zhejiang Province (No. 2005C33026), the Health Foundation of Zhejiang Province (No. 2004ZD00), Zhejiang Province Nature Science Foundation (No. R205120).

References

1. Nam NH (2003) Combretastatin A-4 analogues as antimitotic antitumor agents. Curr Med Chem 10:1697–1722
2. Ohsumi K, Nakagawa R, Fukuda Y et al (1998) Novel combretastatin analogues effective against murine solid tumors, design and structure–activity relationships. J Med Chem 41:3022–3032
3. Cheng Y, Hu Y (2004a) One-pot facile synthesis of 1,3,4-trisubstituted imidazolin-2-ones. J Chem Res 4:292–293
4. Cheng Y, Hu Y (2004b) Synthesis of arylsubstituted imidazolin-2-one analogues. Chin Chem Lett 15:1281–1284
5. Cheng Y, Hu Y, He Q (2005) Synthesis and antitumor activity of arylsubstituted imidazolin-2-one derivatives. Yao Xue Xue Bao 40:711–716
6. Ling YH, Liebes L, Zou Y, Perez-Soler R (2003a) Reactive oxygen species generation and mitochondrial dysfunction in the apoptotic response to Bortezomib, a novel proteasome inhibitor, in human H460 non-small cell lung cancer cells. J Biol Chem 278:33714–33723
7. Ryan L, O'Callaghan YC, O'Brien NM (2005) The role of the mitochondria in apoptosis induced by 7beta-hydroxycholesterol and cholesterol-5beta,6beta-epoxide. Br J Nutr 94:519–525
8. Tang L, Zhang Y (2005a) Mitochondria are the primary target in isothiocyanate-induced apoptosis in human bladder cancer cells. Mol Cancer Ther 4:1250–1259
9. Rosato RR, Almenara JA, Grant S (2003) The histone deacetylase inhibitor MS-275 promotes differentiation or apoptosis in human leukemia cells through a process regulated by generation of reactive oxygen species and induction of $p21^{CIP1/WAF1}$. Cancer Res 63:3637–3645
10. Batra S, Reynolds CP, Maurer BJ (2004) Fenretinide cytotoxicity for Ewing's sarcoma and primitive neuroectodermal tumor cell lines is decreased by hypoxia and synergistically enhanced by ceramide modulators. Cancer Res 64:5415–5424
11. Rotem R, Heyfets A, Fingrut O, Blickstein D, Shaklai M, Flescher E (2005) Jasmonates, novel anticancer agents acting directly and selectively on human cancer cell mitochondria. Cancer Res 65:1984–1993
12. Ogbourne SM, Suhrbier A, Jones B et al (2004) Antitumor activity of 3-ingenyl angelate, plasma membrane and mitochondrial disruption and necrotic cell death. Cancer Res 64:2833–2839
13. Wu CC, Chan ML, Chen WY, Tsai CY, Chang FR, Wu YC (2005) Pristimerin induces caspase-dependent apoptosis in MDA-MB-231 cells via direct effects on mitochondria. Mol Cancer Ther 4:1277–1285
14. Doi S, Soda H, Oka M et al (2004) The histone deacetylase inhibitor FR901228 induces caspase-dependent apoptosis via the mitochondrial pathway in small cell lung cancer cells. Mol Cancer Ther 3:1397–1402
15. Chang L, Karin M (2001) Mammalian MAP kinase signalling cascades. Nature 410:37–40
16. Choi JM, Shin HK, Kim KY, Lee JH, Hong KW (2002) Neuroprotective effect of cilostazol against focal cerebral ischemia via antiapoptotic action in rats. J Pharmacol Exp Ther 300:787–793
17. Ghobrial IM, Witzig TE, Adjei AA (2005) Targeting apoptosis pathways in cancer therapy. CA Cancer J Clin 55:178–194
18. Tang L, Zhang Y (2005b) Mitochondria are the primary target in isothiocyanate-induced apoptosis in human bladder cancer cells. Mol Cancer Ther 4:1250–1259
19. Oliver CL, Miranda MB, Shangary S, Land S, Wang S, Johnson DE (2005) (-)-Gossypol acts directly on the mitochondria to overcome Bcl-2- and Bcl-X(L)-mediated apoptosis resistance. Mol Cancer Ther 4:23–31
20. Miao ZH, Ding J (2003) Transcription factor c-Jun activation represses mdr-1 gene expression. Cancer Res 63:4527–4532
21. Yang B, Reynolds CP (2005) Tirapazamine cytotoxicity for neuroblastoma is p53 dependent. Clin Cancer Res 11:2774–2780
22. Zhou L, Zhu X (2000) Reactive oxygen species-induced apoptosis in PC12 cells and protective effect of bilobalide. J Pharmacol Exp Ther 293:982–988
23. Ling Y, Liebes L, Zou Y, Perez-Soler R (2003b) Reactive oxygen species generation and mitochondrial dysfunction in the apoptotic response to Bortezomib, a novel proteasome inhibitor, in human H460 non-small cell lung cancer cells. J Biol Chem 278:33714–33723
24. Ratajczak MZ, Kant JA, Luger SM et al (1992) In vivo treatment of human leukemia in a scid mouse model with c-myb antisense oligodeoxynucleotides. Proc Natl Acad Sci USA 89:11823–11827
25. Naumovski L, Ramos J, Sirisawad M et al (2005a) Sapphyrins induce apoptosis in hematopoietic tumor-derived cell lines and show in vivo antitumor activity. Mol Cancer Ther 4:968–976
26. Devi GR (2004) XIAP as target for therapeutic apoptosis in prostate cancer. Drug News Perspect 17:127–134
27. Naumovski L, Ramos J, Sirisawad M et al (2005b) Sapphyrins induce apoptosis in hematopoietic tumor-derived cell lines and show in vivo antitumor activity. Mol Cancer Ther 4:968–976
28. Amantana A, London CA, Iversen PL, Devi GR (2004) X-linked inhibitor of apoptosis protein inhibition induces apoptosis and enhances chemotherapy sensitivity in human prostate cancer cells. Mol Cancer Ther 3:699–707
29. Yamanaka K, Rocchi P, Miyake H et al (2005) A novel antisense oligonucleotide inhibiting several antiapoptotic Bcl-2 family members induces apoptosis and enhances chemosensitivity in androgen-independent human prostate cancer PC3 cells. Mol Cancer Ther 4:1689–1698
30. Sinicrope FA, Penington RC (2005) Sulindac sulfide-induced apoptosis is enhanced by a small-molecule Bcl-2 inhibitor and by TRAIL in human colon cancer cells overexpressing Bcl-2. Mol Cancer Ther 4:1475–1483
31. Hayward RL, Macpherson JS, Cummings J, Monia BP, Smyth JF, Jodrell DI (2004) Enhanced oxaliplatin-induced apoptosis following antisense Bcl-xl down-regulation is p53 and Bax dependent, genetic evidence for specificity of the antisense effect. Mol Cancer Ther 3:169–178
32. Katiyar SK, Roy AM, Baliga MS (2005) Silymarin induces apoptosis primarily through a p53-dependent pathway involving Bcl-2/Bax, cytochrome c release, and caspase activation. Mol Cancer Ther 4:207–216

33. Childs AC, Phaneuf SL, Dirks AJ, Phillips T, Leeuwenburgh C (2002) Doxorubicin treatment in vivo causes cytochrome C release and cardiomyocyte apoptosis, as well as increased mitochondrial efficiency, superoxide dismutase activity, and Bcl-2, Bax ratio. Cancer Res 62:4592–4598
34. Cobb MH (1999) MAP kinase pathways. Prog Biophys Mol Biol 71:479–500
35. Xia Z, Dickens M, Raingeaud J, Davis RJ, Greenberg ME (1995) Opposing effects of ERK and JNK-p38 MAP kinases on apoptosis. Science 270:1326–1331
36. Ortiz MA, Lopez-Hernandez FJ, Bayon Y, Pfahl M, Piedrafita FJ (2001) Retinoid-related molecules induce cytochrome c release and apoptosis through activation of c-Jun NH(2)-terminal kinase/p38 mitogen-activated protein kinases. Cancer Res 61:8504–8512
37. Miyoshi N, Uchida K, Osawa T, Nakamura Y (2004) A link between benzyl isothiocyanate-induced cell cycle arrest and apoptosis, involvement of mitogen-activated protein kinases in the Bcl-2 phosphorylation. Cancer Res 64:2134–2142
38. Lewis TS, Shapiro PS, Ahn NG (1998) Signal transduction through MAP kinase cascades. Adv Cancer Res 74:49–139
39. Rice PL, Washington M, Schleman S, Beard KS, Driggers LJ, Ahnen DJ (2003) Sulindac sulfide inhibits epidermal growth factor-induced phosphorylation of extracellular-regulated kinase 1/2 and Bad in human colon cancer cells. Cancer Res 63:616–620
40. Liu YZ, Boxer LM, Latchman DS (1999) Activation of the Bcl-2 promoter by nerve growth factor is mediated by the p42/p44 MAPK cascade. Nucleic Acids Res 27:2086–2090
41. Jost M, Huggett TM, Kari C, Boise LH, Rodeck U (2001) Epidermal growth factor receptor-dependent control of keratinocyte survival and Bcl-xL expression through a MEK-dependent pathway. J Biol Chem 276:6320–6326
42. Capano M, Crompton M (2006) Bax translocates to mitochondria of heart cells during simulated ischaemia, involvement of AMP-activated and p38 mitogen-activated protein kinases. Biochem J 395:57–64
43. Van Laethem A, Van Kelst S, Lippens S et al (2004) Activation of p38 MAPK is required for Bax translocation to mitochondria, cytochrome c release and apoptosis induced by UVB irradiation in human keratinocytes. FASEB J 18:1946–1948